

SUPPORTING INFORMATION

The Interaction of Glycogen Nanoparticles with Human Blood

Nadiia Davydiuk,^{a†} Vaidehi Londhe,^{a†} Manfred F. Maitz,^a Carsten Werner,^a Andreas Fery,^a Quinn A. Besford^{*a}

Supporting Information

Table of Contents

Results and Discussion

Physicochemical properties of source-dependent glycogen NPs (size distribution, PDI, ZP, branching degree)	3
Molecular weight and molar mass determination (GPC)	4
The expression of markers on immune cells with various glycogen NPs and without	5
Immune cell association of silica NPs	6
Immune cell association of glycogen nanoparticles NPs in blood across different donors	7
Coagulation activation of positive controls (kaolin, zymosan, and silica NPs)	8

References	9
------------	---

Results and Discussion

Table S1. The physicochemical properties of source-dependent glycogen NPs.

Sample Name		PG	OG	RLG	BLG
Size (DLS)	d.nm	71.9±0.3	47.8±0.2	43.4±0.3	20.7±0.4
Size (AFM)	d.nm	91.7±16.0	46.7±5.5	66.8±23.8	44.3±16.2
Pdi		0.08±0.01	0.10±0.01	0.17±0.01	0.23±0.04
ZP	mV	-2.23±0.2	-2.29±1.6	-8.08±0.6	-5.26±0.1
Branching degree*	%	7.6±0.3	7.1±0.0	15.6±0.0	8.8±0.0

*the branching degree (data taken from published papers (PG², OG³, RLG¹, BLG¹).

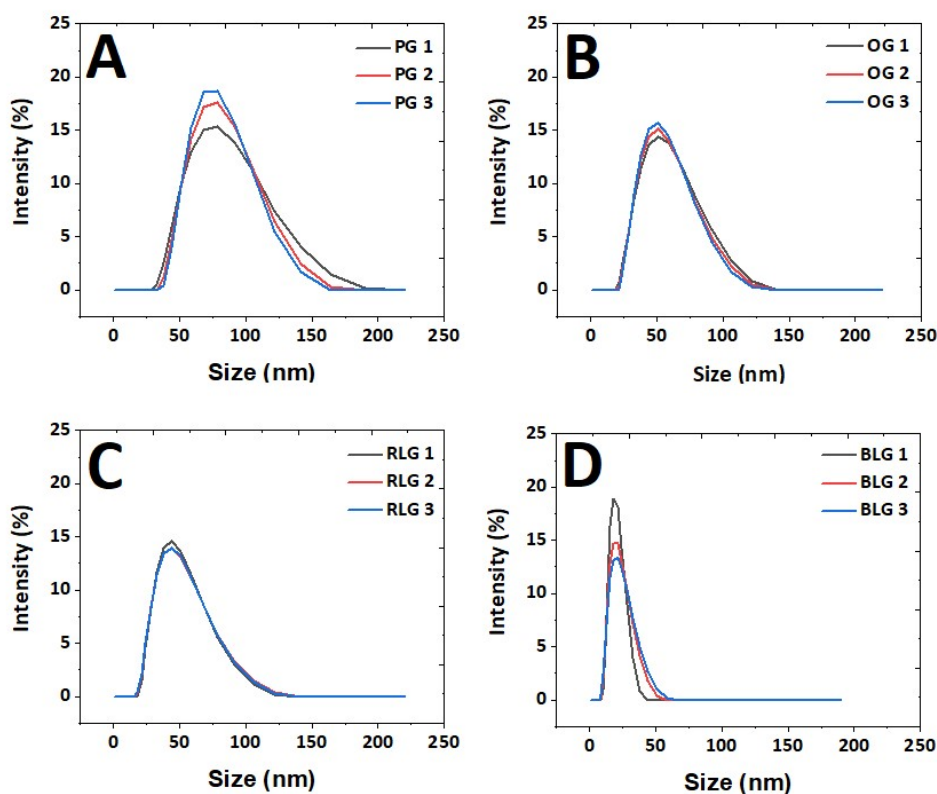


Figure S1. DLS intensity distributions of NPs in MQ-water (pH 5.5) at 25 °C: A) PG, B) OG, C) RLG and D) BLG. For measurements used three replicates of each sample.

Table S2. The molar mass and molecular weight of source-dependent glycogen NPs.

Sample Name		PG	OG	RLG	BLG
Mn	kg/mol	29 050±1 061	6 727±72	4 260±10	203±16
Mw	kg/mol	43 100±1 414	11 200±0	7 150±206	556±10
D	M_w/M_n	1.5±0.0	1.7±0.1	1.7±0.1	2.8±0.9

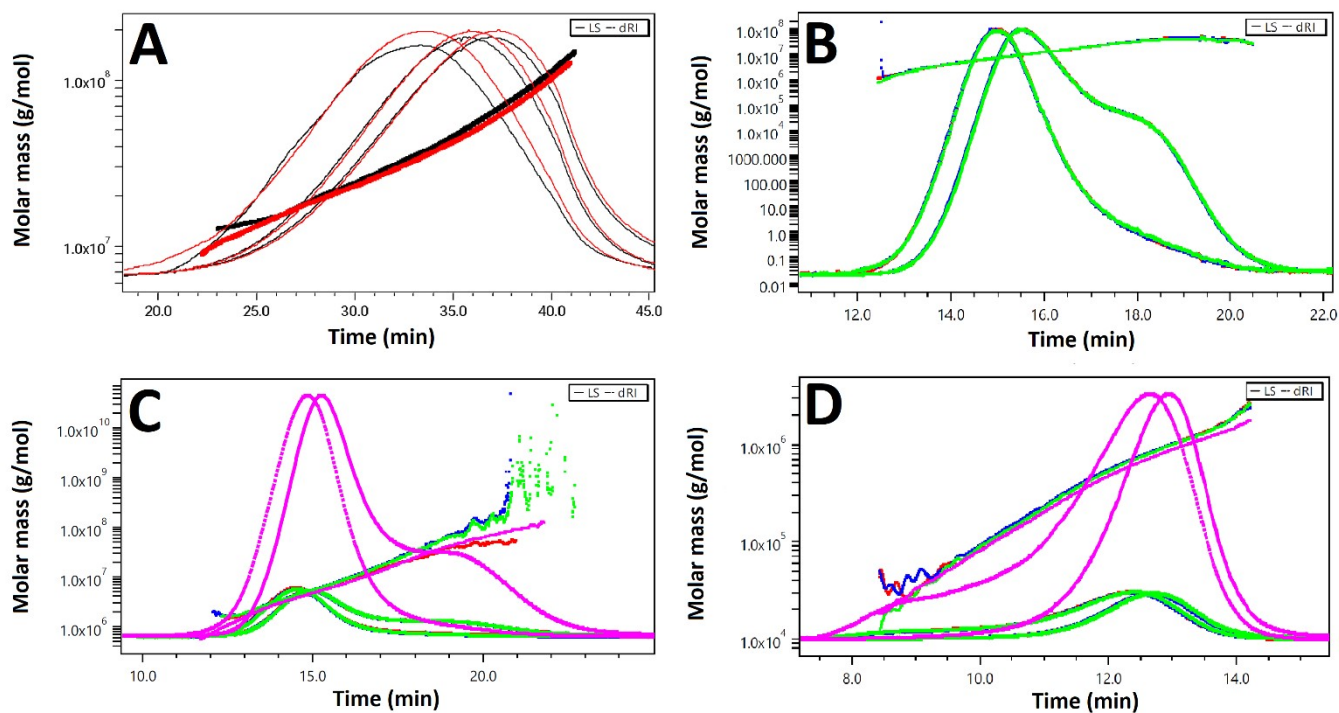


Figure S2. Fractograms of optical separation, RI and LS signal of molar masses: A) PG, B) OG, C) RLG and D) BLG.

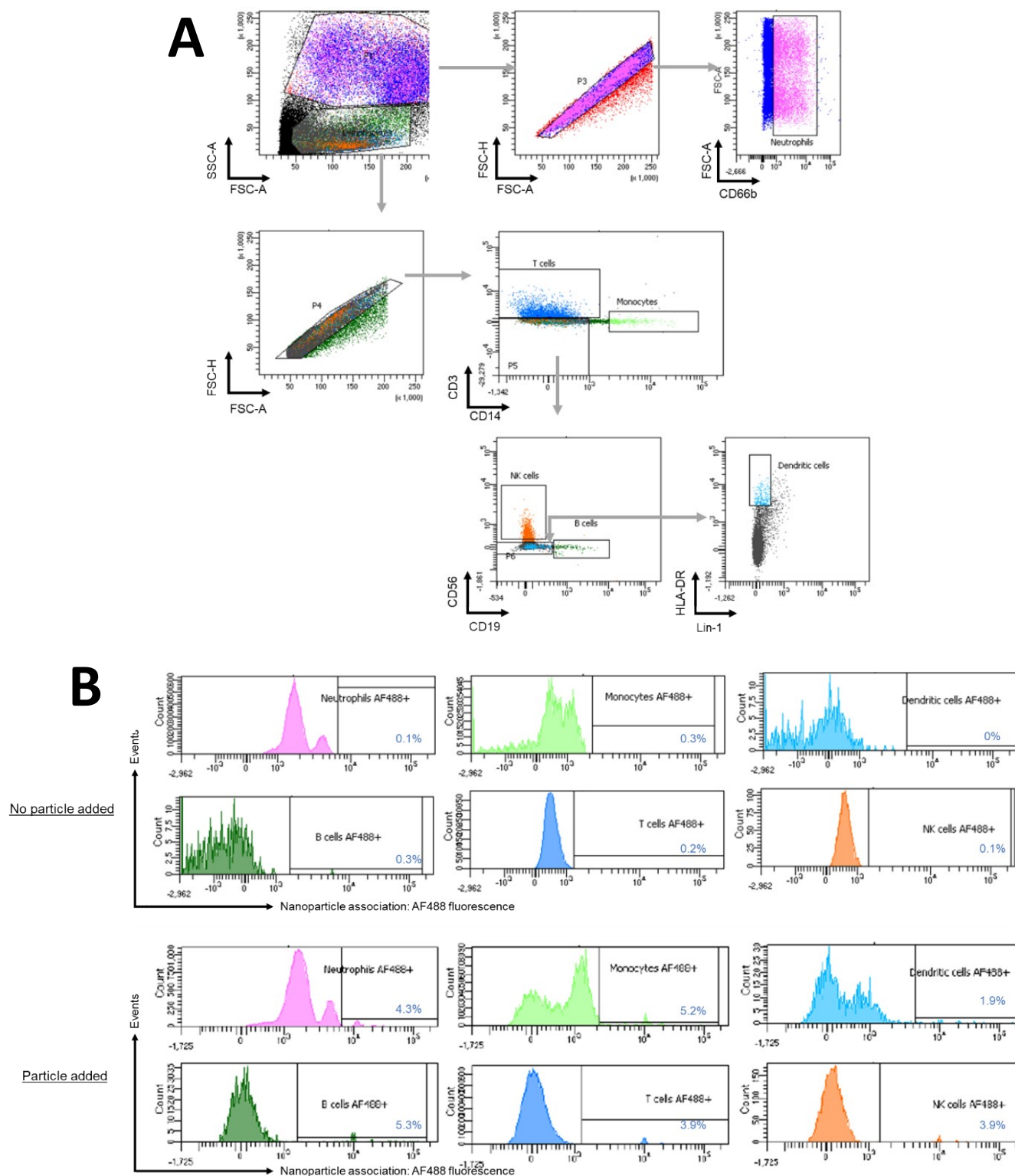


Figure S3. (A) Gating strategy used to identify white blood cell populations. Side and forward scatter were first used to locate white blood cells before doublets were excluded. The following cell types were identified based on expression of surface markers: CD66b+ neutrophils; CD3+ T cells; CD14+ monocytes; CD56+ NK cells; CD19+ B cells and Lin-, HLA-DR+ dendritic cells. (B) The percentage of each cell type positive for the AF488 -NHS labelled particles was then measured and an example of the gating and particle association values for one sample is shown.

SUPPORTING INFORMATION

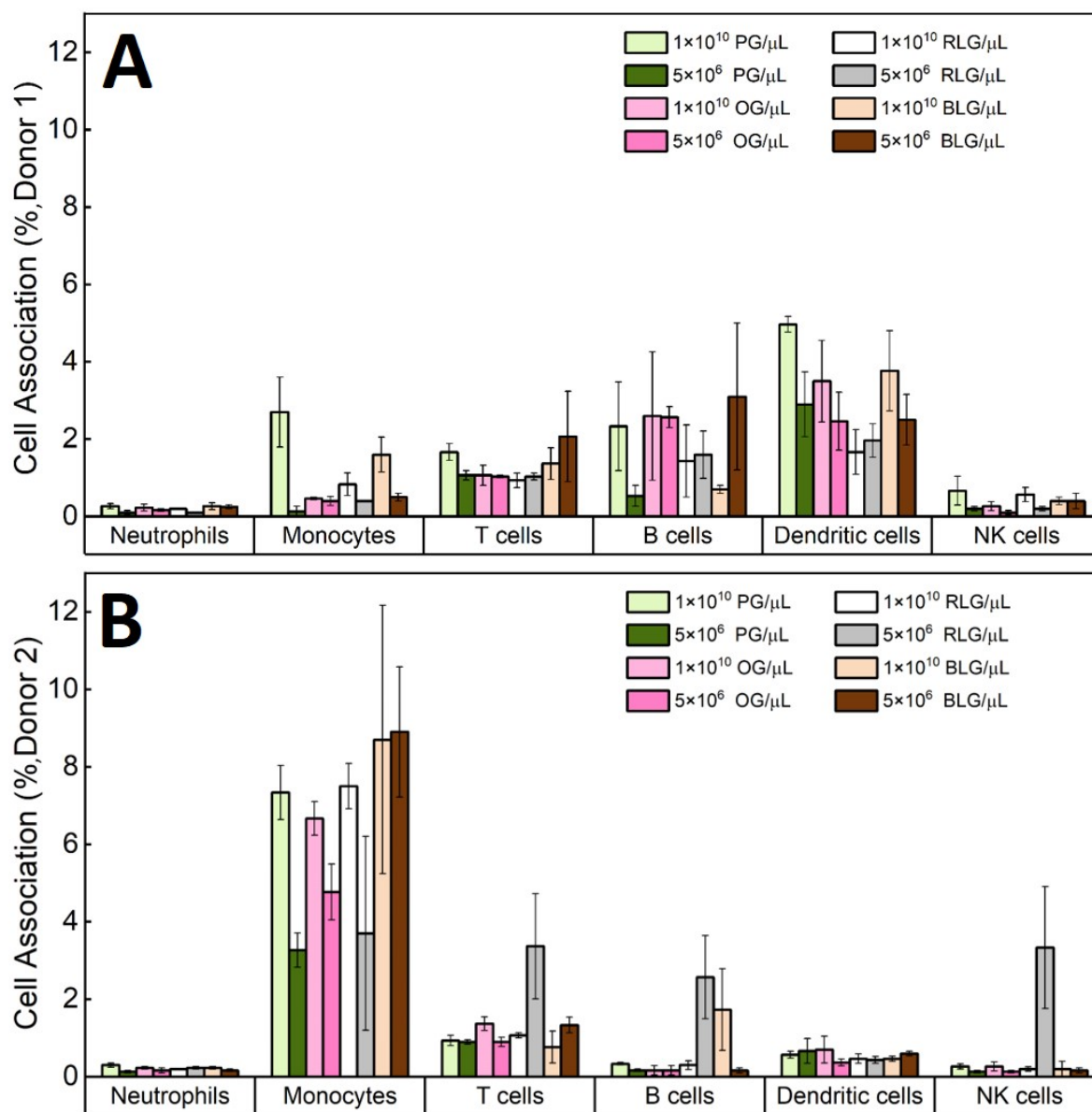


Figure S4. Association of glycogen NPs/ μL with immune cells in blood across different donors.

SUPPORTING INFORMATION

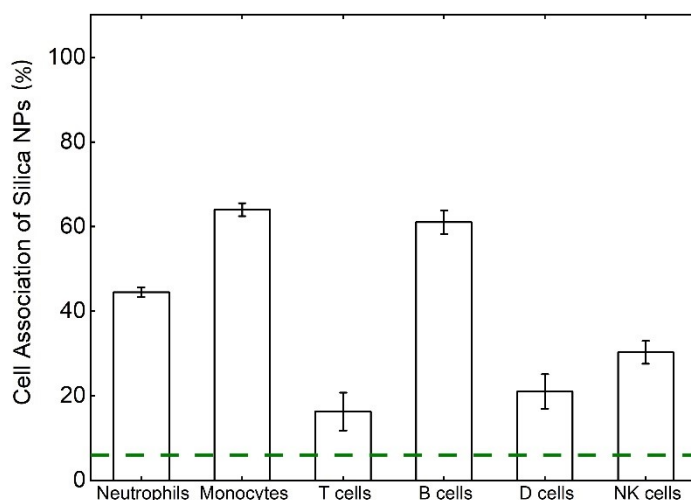


Figure S5. Immune cell association of 1×10^6 silica NPs/ μL labelled with AF488-NHS ($n=3$). Green line indicates the maximum value immune cell-glycogen NP association observed.

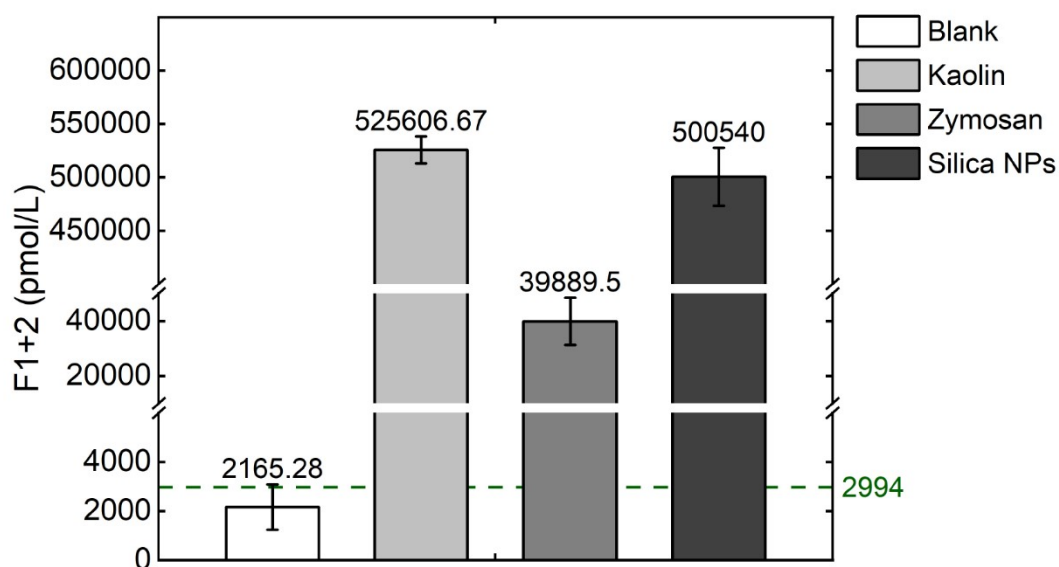


Figure S6. Prothrombin fragment 1 + 2 (F1+2) levels in response to $10 \mu\text{g/ml}$ of kaolin, $10 \mu\text{g/ml}$ zymosan and 1×10^7 silica NPs/ml. Green line indicates the maximum F1+2 value observed with 1×10^{10} and 5×10^6 glycogen NPs/ μL concentration.

SUPPORTING INFORMATION

References

1. M. Wojnilowicz, Q. A. Besford, Y. L. Wu, X. J. Loh, J. A. Braunger, A. Glab, C. Cortez-Jugo, F. Caruso and F. Cavalieri, *Biomaterials*, 2018, **176**, 34-49.
2. X. Jiang, P. Zhang, S. Li, X. Tan, Z. Hu, B. Deng, K. Wang, C. Li, M. A. Sullivan, E. Li and R. G. Gilbert, *Eur. Polym. J.*, 2016, **82**, 175-180.
3. M. Martinez-Garcia, M. C. Stuart and M. J. van der Maarel, *Int. J. Biol. Macromol.*, 2016, **89**, 12-18.